Intermetallic charge-transfer transition in Bi1-xLaxNiO3 as the origin of the colossal negative thermal expansion

Intermetallic charge-transfer transition in $Bi_{1-x}La_xNiO_3$ as the origin of the colossal negative thermal expansion

Kengo Oka,[1,*] Masaichiro Mizumaki,[2] Chika Sakaguchi,[1] Alexandra Sinclair,[3] Clemens Ritter,[4] J. Paul Attfield,[3] and Masaki Azuma[1]

[1]*Materials and Structures Laboratory, Tokyo Institute of Technology, 4259 Nagatsuta, Midori-ku, Yokohama 226-8053, Japan*

[2]*Japan Synchrotron Radiation Research Institute, SPring-8, Sayo-gun, Hyogo 679-5198, Japan*

[3]*Centre for Science at Extreme Conditions and School of Chemistry, University of Edinburgh, Mayfield Road, Edinburgh EH9 3JZ, United Kingdom*

[4]*Institut Laue-Langevin, Boite Postale 156, Grenoble 38042, France*

(Received 18 January 2013; revised manuscript received 3 May 2013; published 29 July 2013)

The nature of triclinic to orthorhombic phase transition, at which colossal negative thermal expansion is observed, and the magnetic ordering of $Bi_{1-x}La_xNiO_3$ have been investigated with neutron powder diffraction (NPD) and x-ray absorption spectroscopy techniques. The presence of a charge-transfer transition from $(Bi/La)^{3+}{}_{0.5}Bi^{5+}{}_{0.5}Ni^{2+}O_3$ to $(Bi/La)^{3+}Ni^{3+}O_3$, accompanied by the simultaneous structural distortion, was confirmed. The NPD data also revealed that magnetic ordering is present only in the insulating triclinic phase. The metallic orthorhombic phase was found to be nonmagnetic down to 10 K.

DOI: 10.1103/PhysRevB.88.014112 PACS number(s): 61.05.F−

I. INTRODUCTION

Variation of valence states can lead to notable phenomena such as superconductivity and magnetoresistance in transition metal oxides. Bismuth is a main group element, but it also has a valence degree of freedom between Bi^{3+} and Bi^{5+} depending on $6s^2$ and $6s^0$ electronic configurations. The perovskite oxide $BiNiO_3$ exhibits an unusual charge distribution of $Bi^{3+}{}_{0.5}Bi^{5+}{}_{0.5}Ni^{2+}O_3$ at ambient conditions.[1] Our previous neutron powder diffraction (NPD)[2] and hard x-ray absorption spectroscopy (XAS)[3] studies revealed a pressure-induced charge transfer between Bi and Ni leading to the valence distribution $Bi^{3+}Ni^{3+}O_3$ at 3.5 GPa. This transition is marked by a simultaneous structural change from a triclinic ($P\bar{1}$) to an orthorhombic ($Pbnm$) $GdFeO_3$-type phase accompanied by a metal-insulator transition[4] and 2.5% volume shrinkage because of the increase in Ni valence from 2+ to 3+.[2] The same transition was found in $Bi_{0.95}La_{0.05}NiO_3$ at ambient pressure.[5] The large triclinic phase and the small orthorhombic phase coexist over a wide temperature range, and the change in their phase fractions with temperature leads to a colossal negative thermal expansion (CNTE) with a measured dilatometric linear thermal expansion coefficient of $-82 \times 10^{-6}\ K^{-1}$ between 320 and 380 K.[6] Further La substitution for Bi leads to increase in the fraction of the orthorhombic phase at room temperature, and the orthorhombic phase becomes dominant above $x = 0.20$.[5] This sample shows a metallic conductivity, suggesting the presence of Ni^{3+}. These behaviors agree with the charge-transfer transition in $BiNiO_3$. However, there are several experimental results inconsistent with the charge-transfer picture. Ni-2p XAS suggested that the valence of Ni in $Bi_{1-x}La_xNiO_3$ was $(2+x)+$ in both triclinic and orthorhombic phases, without a distinct change from 2+ to 3+.[7] In addition, the magnetic transition temperature of $Bi_{1-x}La_xNiO_3$ (x = 0–0.2) was almost independent of the La content despite the $S = 1$ to 1/2 spin state change expected as the Ni valence changes from 2+ to 3+.[1,5] These uncertainties warrant a precise structural analysis of the La-substituted samples, using neutron diffraction to provide precise oxygen positions and magnetic structures, and a hard XAS study to check the soft XAS results.

For this paper, we investigated the temperature evolution of the valence state of $Bi_{1-x}La_xNiO_3$ by means of NPD and Ni-K edge XAS studies. The presence of the charge transfer and the oxidation of Ni from 2+ to 3+ as the origin of the CNTE are confirmed. The metallic orthorhombic $(Bi,La)^{3+}Ni^{3+}O_3$ phase is found to be nonmagnetic, so the antiferromagnetic transition observed by susceptibility measurements is attributed to the coexisting triclinic phase.

II. EXPERIMENTAL DETAILS

Polycrystalline samples of $Bi_{1-x}La_xNiO_3$ (x = 0.05, 0.10, and 0.20) were obtained by high-pressure synthesis as described previously.[1,5,6] Neutron diffraction data were collected from 10 to 500 K at the Institut Laue-Langevin in Grenoble, France, using the high-resolution diffractometer D2B ($\lambda = 1.594$ Å). Further diffraction patterns were measured for the $x = 0.10$ sample on the high-flux D1B ($\lambda = 2.519$ Å) at 10 K. Data analysis was performed by the Rietveld method using the FullProf suite[8] and General Structural Analysis System[9] programs. Hard XAS measurements at the Ni K edge were carried out at the BL01B1 beamline of Super Photon ring-8 (SPring-8), Japan. This beamline is composed of a double monochromator equipped with a Si 111 crystal and Rh-coated double mirror to reduce the higher harmonics with a cutoff energy of 10 keV.[10] The data were collected in the transmission mode from 10 to 498 K using a heater and cryostat. The energy resolution is $< 2 \times 10^{-4}$ around the Ni K edge. XAS spectra were normalized to 1.0 above the edge and analyzed using the Ifeffit software package.[11] The background was fitted using Victoreen's equation and a constant $a/E^3 + b/E^4 + c$, where E is energy and a, b, and c are fitting parameters[12] and are subtracted from XAS spectra. Edge positions were determined as the value of the energy of the arctangent function in least-squares fits of the x-ray absorption near edge structure (XANES) region (<8355 eV)

using an arctangent plus a Gaussian function[13]

$$\frac{1}{\pi}\tan^{-1}\frac{(x-E_0)}{dE}+0.5+\frac{A}{\sqrt{2\pi}\sigma}\exp\left(-\frac{(x-E_1)^2}{2\sigma^2}\right),$$

where x is the x-ray energy in electron volts, E_0 is the absorption edge, dE is the half width of the edge, E_1 is the energy of the white line, σ is the standard deviation, and the A is the fit parameter.

III. RESULTS AND DISCUSSION

Rietveld fits to NPD patterns of $Bi_{1-x}La_xNiO_3$ with $x = 0.05$, 0.10, and 0.20 were performed assuming the presence of a magnetic triclinic phase and a nonmagnetic orthorhombic phase, as described later. Fits to 10 K data are shown in Fig. 1, and crystallographic parameters are summarized in Tables I and II. Fits successfully converged for each temperature and the phase fractions and bond valence sums (BVSs) for Bi and Ni sites using standard Bi^{3+}, Bi^{5+}, Ni^{2+}, and Ni^{3+} parameters, calculated from the refined bond distances are shown in Table III. The BVS parameters demonstrate that the apparent valence distributions are $(Bi/La)^{3+}{}_{0.5}(Bi/La)^{5+}{}_{0.5}Ni^{2+}O_3$ for the triclinic phase and $(Bi/La)^{3+}Ni^{3+}O_3$ for the orthorhombic phase, with little apparent change in the BVS values with x. The fraction of the $(Bi/La)^{3+}Ni^{3+}O_3$ phase increases with increasing temperature, indicating the broad charge-transfer transition. The presence of Bi^{4+}, as suggested in the $Bi^{4+}{}_{1-x}La^{3+}{}_xNi^{(2+x)+}O_3$ valence distribution proposed by the previous Ni-2p XAS,[7] is not supported by the structural results.

The discrepancy between the present NPD results and those of the previous spectroscopic study may be explained through the sensitivity of the Ni-2p XAS to the partial delocalization of the Ni^{3+} charge as a ligand hole. Analysis of the Ni-K XAS data around the pre-edge region led to a description of the Ni^{3+} state in the $BiNiO_3$ high-pressure phase as not purely d^7 but 56% d^7 + 44% d^8L, where L denotes the ligand hole. This effect, and the presence of some triclinic phase containing Ni^{2+}, reduced the energy shift of the Ni-2p absorption and led to the assignment of the Ni valence in $Bi_{1-x}La_xNiO_3$ as $2+x$ instead of 3.

Figure 2(a) shows the temperature variations of the NPD pattern for $x = 0.05$. The temperature dependences of the unit cell volumes, the fraction of the orthorhombic phase, and the weighted average volumes are plotted in Fig. 2(b). The structural transition from the triclinic to the orthorhombic phase was observed in accordance with previous x-ray diffraction

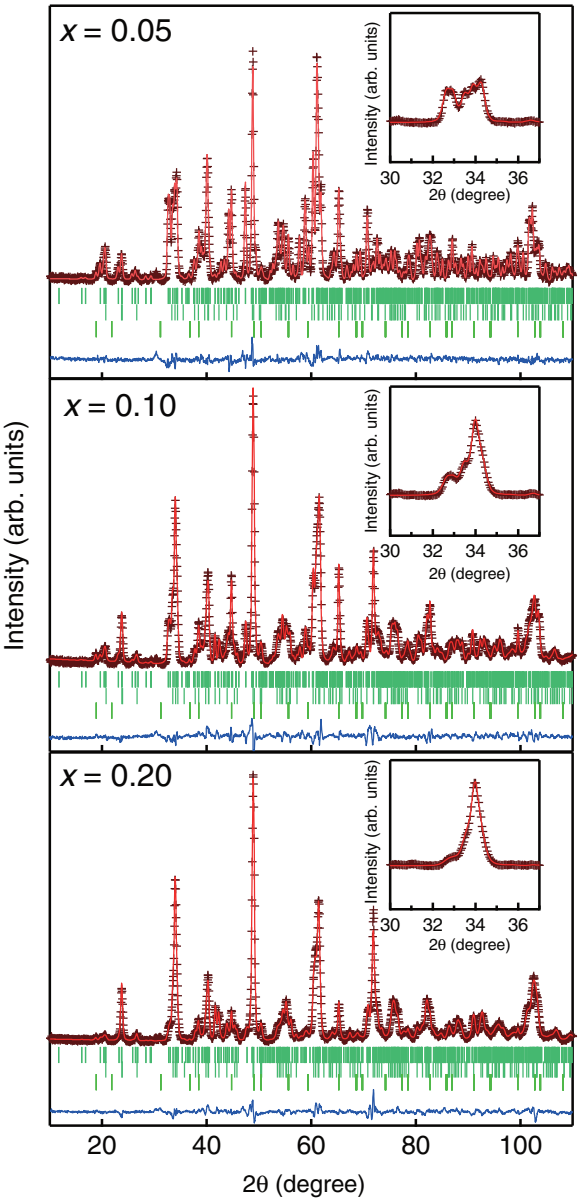

FIG. 1. (Color online) Observed (points), calculated (line), and difference (lower line) patterns from the Rietveld analysis of the NPD data for $Bi_{1-x}La_xNiO_3$ with $x = 0.05$, 0.10, and 0.20 at 10 K ($\lambda = 1.594$ Å). The tick marks correspond to the positions of Bragg reflections of the triclinic phase, the orthorhombic phase, and NiO, from top to bottom. Insets are magnified views of the prominent reflection at $2\theta = 34^\circ$.

TABLE I. Refined lattice parameters at 10 K for $x = 0.05$, 0.10, and 0.20 as upper, middle, and lower values, respectively.[a]

Phase	a (Å)	b (Å)	c (Å)	α (deg.)	β (deg.)	γ (deg.)	V (Å^3)
Triclinic	5.3866(1)	5.6463(1)	7.6955(2)	92.103(2)	89.807(2)	91.632(2)	233.80(1)
	5.3864(4)	5.6436(4)	7.6945(6)	92.025(7)	89.765(7)	91.529(7)	233.67(3)
	5.3721(10)	5.6309(14)	7.7086(16)	91.821(23)	89.730(21)	91.259(20)	233.01(9)
Orthorhombic	5.3577(2)	5.5059(3)	7.6511(3)	90	90	90	225.70(2)
	5.3719(2)	5.4882(2)	7.6561(2)				225.72(1)

[a]Reliability factors for $x = 0.05$ are $R_{WP} = 4.70\%$ and $\chi^2 = 5.360$, for $x = 0.10$ are $R_{WP} = 4.83\%$ and $\chi^2 = 7.769$, and for $x = 0.20$ are $R_{WP} = 4.16\%$ and $\chi^2 = 5.225$.

TABLE II. Crystallographic parameters for $Bi_{1-x}La_xNiO_3$ at 10 K showing refined variables (coordinates and isotropic U factors) and residuals for $x = 0.05$, 0.10, and 0.20 as upper, middle, and lower values, respectively.

Atom	Site	x	y	z	100 Uiso (Å^2)
			Triclinic Phase (S.G. $P-1$)		
Bi/La1	2i	0.0086(3)	0.0509(3)	0.2338(3)	0.69(2)
		0.0060(13)	0.0513(9)	0.2367(8)	0.28(5)
		0.0068(13)	0.0491(13)	0.2320(13)	0.64(9)
Bi/La2	2i	0.5118(3)	0.4439(3)	0.7255(3)	0.69
		0.5100(13)	0.4421(10)	0.7283(7)	0.28
		0.5135(10)	0.4456(10)	0.7272(10)	0.64
Ni1	1d	0.5	0	0	0.52(2)
					0.40(3)
					0.47(5)
Ni2	1c	0	0.5	0	0.52
					0.40
					0.47
Ni3	1f	0.5	0	0.5	0.52
					0.40
					0.47
Ni4	1g	0	0.5	0.5	0.52
					0.40
					0.47
O1	2i	−0.141(1)	0.470(1)	0.253(1)	0.92(2)
		−0.140(2)	0.472(2)	0.255(2)	0.73(4)
		−0.145(4)	0.474(4)	0.253(3)	0.79(6)
O2	2i	0.395(1)	0.076(1)	0.759(1)	0.92
		0.397(2)	0.072(2)	0.757(1)	0.73
		0.396(4)	0.078(3)	0.759(3)	0.79
O3	2i	0.832(1)	0.174(1)	−0.032(1)	0.92
		0.834(2)	0.174(2)	−0.035(1)	0.73
		0.836(4)	0.181(3)	−0.039(2)	0.79
O4	2i	0.318(1)	0.334(1)	0.081(1)	0.92
		0.322(2)	0.335(2)	0.082(1)	0.73
		0.327(5)	0.343(4)	0.076(3)	0.79
O5	2i	0.208(1)	0.766(1)	0.415(1)	0.92
		0.212(2)	0.764(2)	0.410(1)	0.73
		0.213(4)	0.775(4)	0.407(3)	0.79
O6	2i	0.675(1)	0.689(1)	0.546(1)	0.92
		0.675(2)	0.689(2)	0.552(1)	0.73
		0.664(4)	0.690(4)	0.552(3)	0.79
			Orthorhombic Phase (S.G. *Pbnm*)		
Bi	4c	−0.0040(10)	0.0483(4)	0.25	1.21(4)
		−0.0021(2)	0.0431(2)		1.03(4)
Ni	4b	0.5	0	0	
					0.68(3)
					0.33(1)
O1	4c	0.0811(8)	0.4780(8)	0.25	1.32(5)
		0.0716(5)	0.4835(5)		1.01(4)
O2	8d	0.7040(6)	0.2943(6)	0.0403(4)	1.32
		0.7088(4)	0.2898(3)	0.0395(2)	1.01

S.G., space group; Uiso, isotropic U factor.

studies.[5] The transition of $x = 0.05$ is broad compared with the previous reports and is not complete even at 500 K. This is probably due to minor compositional differences among samples. As the NPD measurements required a large amount of sample, capsules 5.6 mm in diameter and 8.0 mm in height were used for the high-pressure syntheses of the NPD samples, while the capsule size for previous samples was 3.6 mm in diameter and 5.0 mm in height. The presence of a pressure or temperature gradient in the larger capsules may have affected the homogeneity of the Bi/La distribution. As the La content increases, the transition is shifted to the lower temperature and the slopes of the phase fractions change become gradual. At $x = 0.20$, the fraction of the orthorhombic phase was almost temperature independent. Since La^{5+} is not formed,

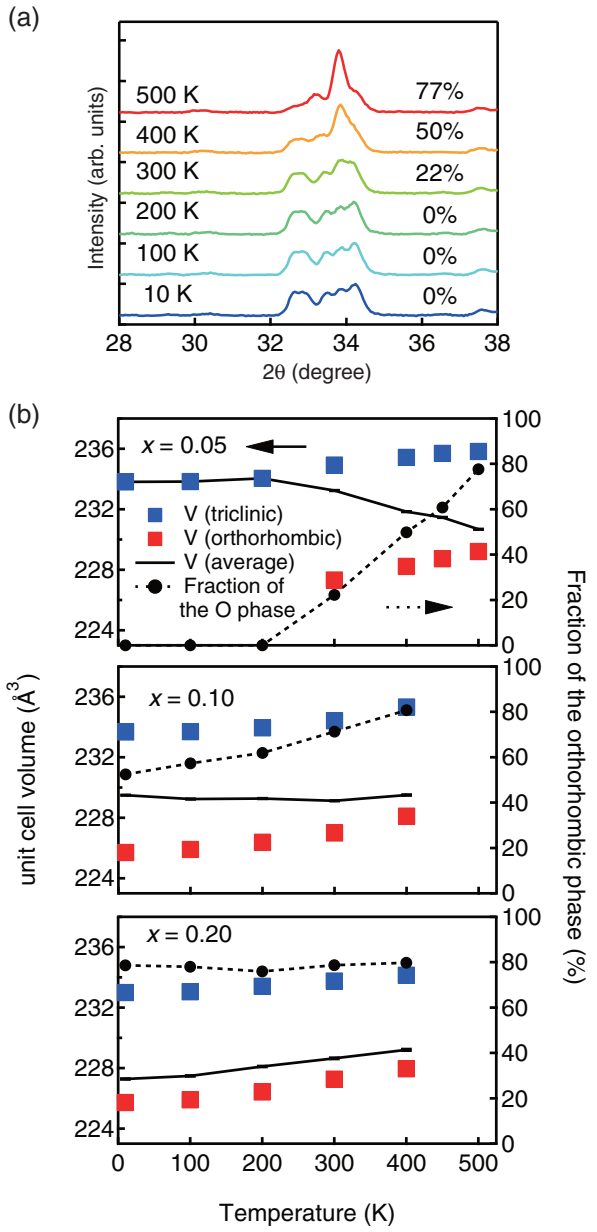

FIG. 2. (Color online) (a) Temperature variations of the NPD pattern for $x = 0.05$ ($\lambda = 1.594$ Å). The labels show the temperature and the phase fraction of the orthorhombic phase. (b) Temperature dependences of the unit cell volumes of the triclinic and orthorhombic phases, the phase fraction of the orthorhombic phase, and the weighted average volume of $Bi_{1-x}La_xNiO_3$ with $x = 0.05$, 0.10, and 0.20.

La ions introduced into the Bi^{5+} site destabilize the valence disproportionation of Bi. The fraction of the triclinic phase therefore decreases, and the orthorhombic phase becomes dominant.

The charge transfer was further confirmed by the hard XAS data. Figure 3(a) shows the XAS spectrum for $Bi_{0.95}La_{0.05}NiO_3$ at 10 K and the fitting result. An arctangent plus a Gaussian function agrees well with the XANES region of the observed data and gives reasonable absorption edge energy. Figure 3(b) shows the temperature dependence around the Ni K edge for $Bi_{1-x}La_xNiO_3$ with $x = 0.05$, 0.10, and 0.20. For $x = 0.05$ and

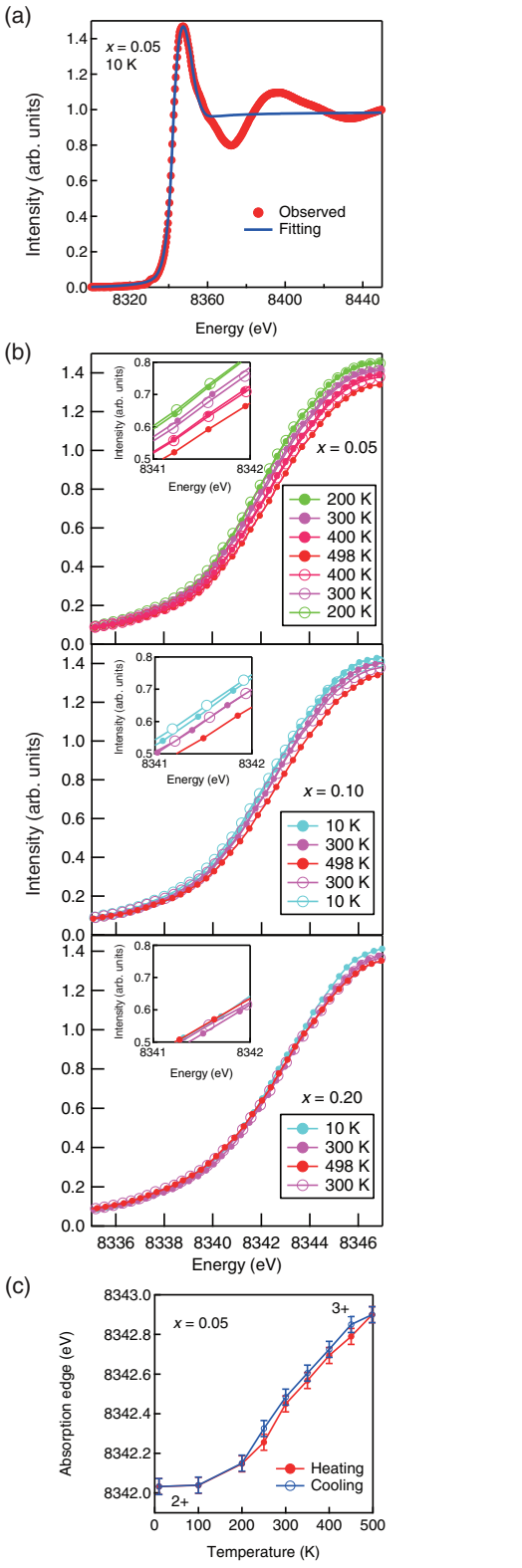

FIG. 3. (Color online) (a) XAS spectra for $Bi_{0.95}La_{0.05}NiO_3$ at 10 K and the fitting result. (b) Temperature dependence around the Ni K edge for $Bi_{1-x}La_xNiO_3$ with $x = 0.05$, $x = 0.10$, and $x = 0.20$. Insets show magnified views. Solid and open circles represent heating and cooling processes, respectively. (c) Temperature dependence of absorption edge energy around Ni K XAS spectra for $x = 0.05$. The mechanical accuracy of the monochromator (± 0.04 eV) is shown as error bars.

TABLE III. Phase fractions and BVSs for $Bi_{1-x}La_xNiO_3$ at various temperatures. The BVSs for Bi/La sites were calculated using the parameter for Bi^{3+} or Bi^{5+} ions. Approximately 1 wt% of impurity NiO was found for all samples.

	Triclinic phase							Orthorhombic phase			NiO
Temperature (K)	Fraction (wt%)	Bi/La1	Bi/La2	Ni1	Ni2	Ni3	Ni4	Fraction (wt%)	Bi/La	Ni	Fraction (wt%)
					$x = 0.05$						
10	99	3.20	4.64	1.93	1.94	1.93	2.13	0			1
300	77	3.17	4.60	1.91	1.93	1.82	2.11	22	3.20	3.10	1
400	49	3.13	4.57	1.90	1.92	2.03	2.10	50	3.18	3.07	1
500	22	3.14	4.56	1.91	1.89	1.81	2.11	77	3.05	2.66	1
					$x = 0.10$						
10	47	3.21	4.73	1.86	1.89	1.90	2.08	52	3.06	2.78	1
300	28	2.77	4.61	1.92	1.93	1.83	2.12	71	3.11	3.21	1
400	19	3.15	4.67	1.90	1.91	1.81	2.11	80	2.97	2.72	1
					$x = 0.20$						
10	20	3.24	4.95	1.84	2.01	1.79	1.88	79	2.92	3.37	1
300	21	3.21	4.63	1.92	1.94	1.84	2.17	78	2.88	3.34	1
400	20	3.20	4.62	1.92	1.94	1.84	2.13	79	2.85	2.79	1

0.10, the absorption edge shifts to higher energy on heating, indicating the increase in Ni valence accompanying the charge-transfer transition. This behavior is essentially the same as that observed for $BiNiO_3$ under pressure.[3] The shift for $x = 0.10$ is 40% of that of $x = 0.05$, reflecting the difference in the change of the orthorhombic phase fraction as plotted in Fig. 2(b), and for $x = 0.20$, the absorption edge is almost temperature independent. The results of XAS measurements indicate that the valence of Ni changes from 2+ for the triclinic phase to 3+ for the orthorhombic phase, supporting the NPD results. Figure 3(c) shows the temperature dependence of the absorption edge energy for $x = 0.05$, confirming a reversible charge-transfer transition showing hysteresis in accordance with the CNTE observed for $x = 0.05$.[6]

The magnetic structures of the triclinic and orthorhombic phases were analyzed to discover whether the G-type antiferromagnetic ordering found in the parent compound, triclinic $BiNiO_3$, persists in the $Bi_{1-x}La_xNiO_3$ derivatives.[14] Figure 4 shows a magnified view of the NPD pattern of $x = 0.10$ collected on diffractometer D1B at 10 K, where the weight fractions of the triclinic and orthorhombic phases were 47% and 52%, respectively. Although the G-type antiferromagnetic ordering does not give further Bragg reflections because it has the same $\sqrt{2}a \times \sqrt{2}a \times 2a$ supercell as both triclinic and orthorhombic forms of $BiNiO_3$, where a is the lattice constant of a cubic perovskite, the magnetic component is evident from the intensities of NPD peaks. G-type antiferromagnetic ordering in the orthorhombic phases would add intensity at $2\theta = 33.4^\circ$ (011 reflection), but there is no observed magnetic contribution. Refinements gave correspondingly small magnetic moments of $<0.1\ \mu_B$ for the orthorhombic $Bi_{1-x}La_xNiO_3$ components, demonstrating the nonmagnetic nature of this metallic orthorhombic phase. In contrast, the ordered magnetic moments per Ni in the triclinic phases at 10 K are 1.66(4) μ_B for $x = 0.05$, 1.72(6) μ_B for $x = 0.10$, and 1.64(11) μ_B for $x = 0.20$, close to that of triclinic $BiNiO_3$ (1.74(3) μ_B at 5 K)[14] containing Ni^{2+} ($S = 1$). The temperature dependence of the magnetic moment of Ni^{2+} in the triclinic phase is shown in Fig. 5 and is similar to that of the magnetic susceptibility.[5] The charge-transfer and magnetic transitions of $Bi_{1-x}La_xNiO_3$ occur separately (e.g., at 200–500 K and 330 K, respectively, for $x = 0.05$), and from the present NPD results, it is clear that the magnetic transition is due to spin order in the triclinic phase.

The XAS and NPD results both confirm the existence of a temperature- and composition-induced intermetallic charge transfer in $Bi_{1-x}La_xNiO_3$. The transition is of the first order, and the A-site Bi-disproportionated triclinic phase and $(Bi,La)^{3+}Ni^{3+}O_3$ orthorhombic phase coexist in the investigated samples. This is in contrast to the situation in $SrCu_3Fe_4O_{12}$,[15] where a similar temperature-induced Cu

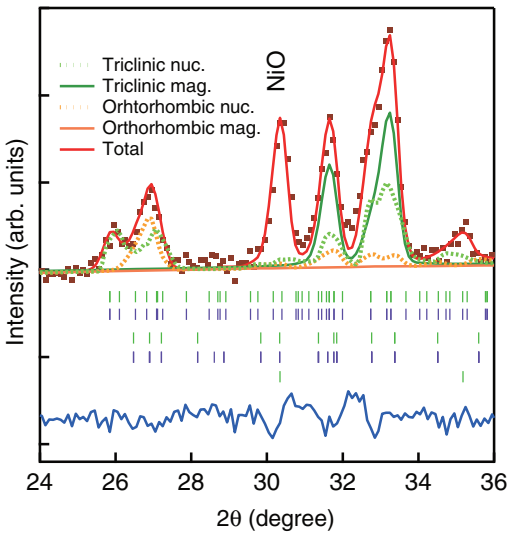

FIG. 4. (Color online) Magnified region of the NPD pattern of the $x = 0.10$ sample at 10 K ($\lambda = 2.519$ Å). Observed (points), calculated (fitted lines), and difference (lower line) profiles of the Rietveld analysis are shown. The nuclear and magnetic contributions from the triclinic and the orthorhombic phases are indicated. The tick marks represent the reflections of the crystal and magnetic structures of the triclinic and orthorhombic phases and NiO, shown from top to bottom.

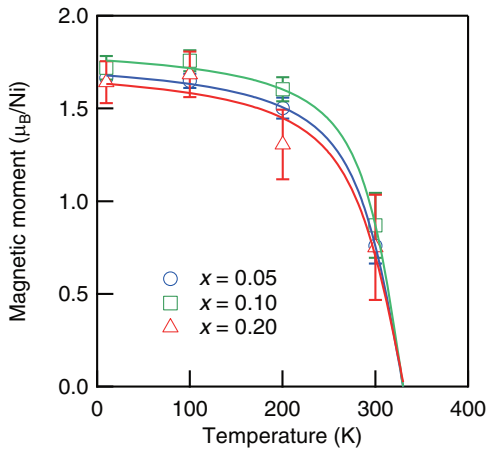

FIG. 5. (Color online) The evolution of the ordered Ni magnetic moment for the triclinic phase as a function of temperature in $Bi_{1-x}La_xNiO_3$ with $x = 0.05$, 0.10, and 0.20.

to Fe charge transfer exists but the lattice parameter and the Fe isomer shift change smoothly. The first-order charge transfer in $Bi_{1-x}La_xNiO_3$ can be attributed to Bi^{3+}/Bi^{5+} valence fluctuations, as the intermediate Bi^{4+} state with $6s^1$ electronic configuration is unstable. Hence, the average $Bi^{4+}{}_{1-x}La^{3+}{}_xNi^{(2+x)+}O_3$ valence state previously proposed from Ni-2p XAS results is not plausible.

IV. CONCLUSIONS

The charge distributions of $Bi_{1-x}La_xNiO_3$ were confirmed to be $(Bi/La)^{3+}{}_{0.5}Bi^{5+}{}_{0.5}Ni^{2+}O_3$ for the triclinic phase and $(Bi/La)^{3+}Ni^{3+}O_3$ for the orthorhombic phase. The fraction of the orthorhombic phase increases with heating, accompanied by a simultaneous shift in the Ni-K edge XAS. This indicates that the charge-transfer transition is the origin of the CNTE. An increase in the La concentration x stabilizes the orthorhombic phase. The temperature range of the transition becomes greater with increasing x, and the phase fractions are almost temperature independent at $x = 0.20$. The magnetic transition observed for $Bi_{1-x}La_xNiO_3$ is attributed to just the insulating triclinic phase, as the metallic orthorhombic phase was found to be nonmagnetic.

ACKNOWLEDGMENTS

This paper was supported by the Cabinet Office of the Government of Japan through its "Funding Program for Next Generation World-Leading Researchers" (Contract No. GR032), and a grant-in-aid from the Murata Science Foundation. The NPD experiment was done at the Institut Laue-Langevin. The XAS experiment was conducted at BL01B1 of SPring-8 with the approval of the Japan Synchrotron Radiation Research Institute (Contract No. 2012A1629). J.P.A. thanks the Engineering and Physical Sciences Research Council and the Royal Society for support.

*Corresponding author: koka@msl.titech.ac.jp

[1]S. Ishiwata, M. Azuma, M. Takano, E. Nishibori, M. Takata, M. Sakata, and K. Kato, J. Mater. Chem. **12**, 3733 (2002).
[2]M. Azuma, S. Carlsson, J. Rodgers, M. G. Tucker, M. Tsujimoto, S. Ishiwata, S. Isoda, Y. Shimakawa, M. Takano, and J. P. Attfield, J. Am. Chem. Soc. **129**, 14433 (2007).
[3]M. Mizumaki, N. Ishimatsu, N. Kawamura, M. Azuma, Y. Shimakawa, M. Takano, and T. Uozumi, Phys. Rev. B **80**, 233104 (2009).
[4]S. Ishiwata, M. Azuma, and M. Takano, Solid State Ionics **172**, 569 (2004).
[5]S. Ishiwata, M. Azuma, M. Hanawa, Y. Moritomo, Y. Ohishi, K. Kato, M. Takata, E. Nishibori, M. Sakata, I. Terasaki, and M. Takano, Phys. Rev. B **72**, 045104 (2005).
[6]M. Azuma, W. Chen, H. Seki, M. Czapski, S. Olga, K. Oka, M. Mizumaki, T. Watanuki, N. Ishimatsu, N. Kawamura, S. Ishiwata, M. G. Tucker, Y. Shimakawa, and J. P. Attfield, Nat. Comm. **2**, 347 (2011).
[7]H. Wadati, M. Takizawa, T. T. Tran, K. Tanaka, T. Mizokawa, A. Fujimori, A. Chikamatsu, H. Kumigashira, M. Oshima, S. Ishiwata, M. Azuma, and M. Takano, Phys. Rev. B **72**, 155103 (2005).
[8]J. Rodríguez-Carvajal, Phys. B **192**, 55 (1993).
[9]A. C. Larson and R. B. Von Dreele, General Structural Analysis System (GSAS), Los Alamos National Laboratory Report 86-748 (Los Alamos National Laboratory, Los Alamos, NM, 2000).
[10]T. Uruga, H. Tanida, Y. Yoneda, K. Takeshita, S. Emura, M. Takahashi, M. Harada, Y. Nishihata, Y. Kubozono, T. Tanaka, T. Yamamoto, H. Maeda, O. Kamishima, Y. Takabayashi, Y. Nakata, H. Kimura, S. Goto, and T. Ishikawa, J. Synchrotron Radiat. **6**, 143 (1999).
[11]M. Newville, J. Synchrotron Radiat. **8**, 322 (2001).
[12]J. A. Victoreen, J. Appl. Phys. **14**, 95 (1943).
[13]R. Revel, C. Den Auwer, C. Madic, F. David, B. Fourest, S. Hubert, J. F. Le Du, and L. R. Morss, Inorg. Chem. **38**, 4139 (1999).
[14]S. J. E. Carlsson, M. Azuma, Y. Shimakawa, M. Takano, A. Hewat, and J. P. Attfield, J. Solid State Chem. **181**, 611 (2008).
[15]I. Yamada, K. Tsuchida, K. Ohgushi, N. Hayashi, J. Kim, N. Tsuji, R. Takahashi, M. Matsushita, N. Nishiyama, T. Inoue, T. Irifune, K. Kato, M. Takata, and M. Takano, Angew. Chem. Int. Ed. **50**, 6579 (2011).